

Supporting Information

Cyclic conductance switching in networks of redox-active molecular junctions.

Jianhui Liao,[†] Jon S. Agustsson,[†] Songmei Wu,[†] Christian Schönenberger,[†]
Michel Calame,^{*,†} Yann Leroux,[‡] Marcel Mayor,[‡] Olivier Jeannin,[¶] Ying-Fen Ran,[¶]
Shi-Xia Liu,^{*,¶} and Silvio Decurtins[¶]

*Department of Physics, University of Basel, Klingelbergstrasse 82, CH-4056, Basel, Switzerland,
Department of Chemistry, University of Basel, St. Johannis Ring 19, CH-4056 Basel, Switzerland,
and Department of Chemistry and Biochemistry, University of Bern, Freiestrasse 3, CH-3012
Bern, Switzerland*

E-mail: michel.calame@unibas.ch; liu@iac.unibe.ch

*To whom correspondence should be addressed

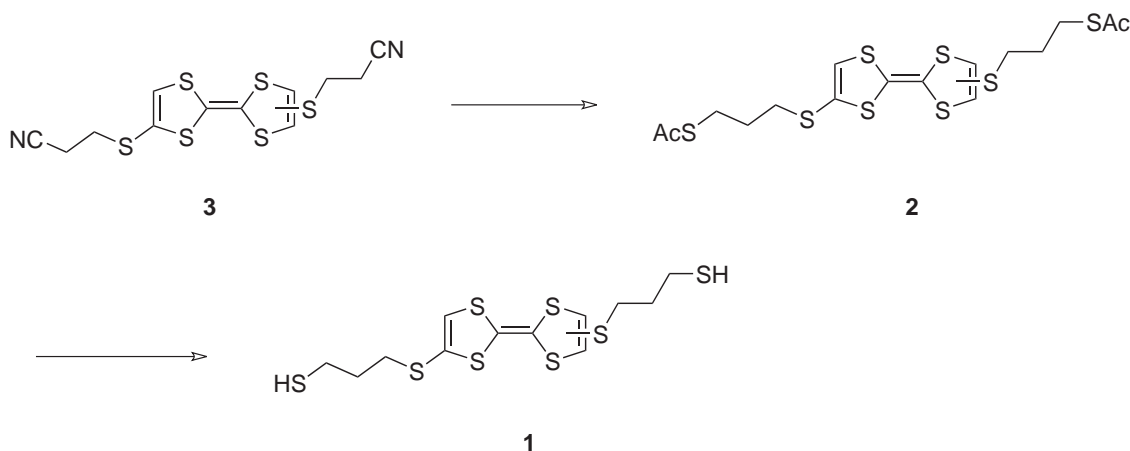
[†]Department of Physics, University of Basel, Klingelbergstrasse 82, CH-4056, Basel, Switzerland

[‡]Department of Chemistry, University of Basel, St. Johannis Ring 19, CH-4056 Basel, Switzerland

[¶]Department of Chemistry and Biochemistry, University of Bern, Freiestrasse 3, CH-3012 Bern, Switzerland

We provide here synthesis details for the tetrathiafulvalene dithiol derivative, a materials and methods section as well as six figures showing additional characterization and control experiments.

Synthesis details



A mixture of cyanoethyl-protected TTF **3**¹ (0.3 g, 0.8 mmol) and CsOH·H₂O (0.27 g, 1.6 mmol) in 10 ml of DMF was stirred for 1 h under nitrogen. Then, 1-iodo-3-thioacetyl propane (0.62 g, 2.4 mmol) was added. After stirring for 2 h, water was added. The resulting solution was extracted with CH₂Cl₂ for several times and the combined organic layers were dried over MgSO₄. The crude product was chromatographed (SiO₂/CH₂Cl₂) to yield compound **2** (0.2 g, 46%) as an orange-yellow oil.

¹H NMR (300 MHz, CDCl₃) δ 6.32 (s, 2H), 2.91 (m, 4H), 2.69 (m, 4H), 2.27 (s, 6H), 1.83 (m, 4H).

Thioacetyl derivative **2** (31 mg, 5.81 · 10⁻² mmol) was dissolved in dry CH₂Cl₂ (10 mL) and cooled at -78°C. A solution of diisobutylaluminium hydride (DIBAL-H) (1 M in toluene, 0.45 mmol) was then added dropwise. After stirring for 45 min at -78°C, the reaction mixture was treated with a chlorhydric acid solution (3 M) in methanol. At room temperature, CH₂Cl₂ (15 mL) were added. The organic phase was washed with water and dried over MgSO₄. After evaporation

of the solvents, the residue was chromatographed on SiO₂ gel (pentane/CH₂Cl₂ 2:1) and afforded **1** (15 mg, 75%) as a yellow oil.

¹H NMR (300 MHz, CDCl₃) δ 6.30 (s, 2H), 2.80 (m, 4H), 2.58 (m, 4H), 1.87 (m, 4H), 1.29 (m, 2H).

Materials and methods

The two-dimensional Au nanoparticle arrays were prepared following a protocol described previously.²⁻⁴ Briefly, alkanethiol-coated Au nanoparticles were self-assembled at the air/water interface and transferred to a Silicon substrate via micro-contact printing.^{5,6} Typically, 10ml of an aqueous gold colloid ($\approx 10\text{nm}$) suspension (concentration $\sim 10^{12}$ particles/ml) was transferred from water to ethanol by centrifugation. The gold colloids were then capped with octanethiols (C8, >98%) by mixing 10ml gold colloids in ethanol with 200 μl C8 molecules. The reaction was carried overnight and resulted in a precipitation of the C8-capped nanoparticle to the bottom of the container. The precipitated product was washed by ethanol to remove excess C8 molecules and dispersed in 4ml chloroform by ultrasonic treatment for 10min. All chemicals were purchased from Fluka and used as received. In order to prepare 2D nanoparticle films, 400 μl of the C8-capped gold nanoparticle solution was cast onto a convex water surface. After the evaporation of the solvent, the nanoparticles self-assembled into 2D arrays. A polydimethylsiloxane (PDMS) stamp with embossed line structures was used to transfer the 2D nanoparticle arrays from the water surface onto a SiO₂/Si substrate and form patterned nanoparticle arrays.

To measure the conductance through the arrays, a transmission electron microscopy (TEM) grid was used as a shadow mask to evaporate Ti/Au (5nm/45nm) contact pads. we refer to each pair of neighboring contact pads with a nanoparticle array between them as a *device* (Figure 1a).

All conductance measurements were carried out in air at room temperature using a probe station. Typically, a bias voltage of up to 10V was applied and the IV characteristics of the devices measured. Because each device consists of a large number of nanoparticles (about 10^6), the voltage drop over neighboring nanoparticles is small and we measure the linear response of the arrays.²

UV-visible absorption was used to probe the change of oxidation states of the TTF groups in solution. In order to prevent a reaction between free thiol groups and the added chemicals, acetyl-protected TTFdT (see Supporting Information) was used for absorption measurements. The original acetyl-protected TTFdT was dissolved in acetonitrile. Different amounts of oxidant (iron(III)chloride, $(\text{FeCl}_3 \cdot 6\text{H}_2\text{O})$) and reductant (ferrocene, $(\text{Fe}(\text{C}_5\text{H}_5)_2)$) were added to the solution.

The dithiolated molecules were inserted into the C8-capped nanoparticle arrays by place-exchange.^{7,8} Typically, the devices were immersed in the solution containing 1mM dithiolated molecules in THF for 24 hours. The devices were then rinsed in tetrahydrofuran (THF) and dried with nitrogen gas. During the course of immersion, new dithiolated molecules partially displace C8 molecules^{2,3} and interlink neighboring nanoparticles, resulting in networks of molecular junctions.⁴ Performing the exchange over 24 hours ensures that most neighboring nanoparticles in the device are interlinked by dithiolated molecules. This is evidenced by a saturation of the device conductance as a function of exchange time and becomes manifest after a few hours already.²

The oxidation and reduction of TTFdT after exchange were performed in solution. The sample was immersed in 10ml 10mM solution of iron chloride dissolved in deionized water for 40 minutes to carry out the oxidation. The sample was then taken out and rinsed several time in deionized water and dried with nitrogen gas. To reduce the TTF groups, the sample was immersed in 10ml 10mM ferrocene in THF for several hours to achieve a complete reaction.

For the self-assembled monolayer experiments, we used 2-mm-diameter rod gold electrodes purchased commercially (Metrohm Schweiz AG), which were polished successively in 1.0, 0.3, and 0.05 μm alumina slurry made from dry alumina powder and Milli-Q water on microcloth pads (CH Instruments, Inc. Tx, USA). The electrodes were thoroughly rinsed with Milli-Q water and sonicated in Milli-Q water for 5 min between polishing step. Prior to the SAM formation, the gold surfaces were cleaned using a hot piranha solution (3:1 mixture of concentrated H_2SO_4 and 30% H_2O_2), followed by excessively rinsing with water and ethanol and subsequent drying in an argon stream. Immediately after the cleaning procedure the gold electrodes were immersed in an argon degassed ethanoic solution of 1 mM of TTFdT (molecule 1) for at least 24 hours. The modified gold electrodes were copiously rinsed with ethanol and acetone to remove adsorbed species. The electrochemical measurement were performed in a conventional three-electrode system, using a platinum electrode or a gold modified electrode as working electrode, a platinum foil as the auxiliary electrode, and an Ag/AgCl 3.0 M KCl electrode (Metrohm) as reference. All potentials are reported versus Ag/AgCl reference at room temperature.

As displayed in Figure S4, the redox behavior of these functionalized electrode surfaces is considerably more complicated with respect to the dissolved parent species. Only in the first scan an intense peak at nearly 930 mV with a broad shoulder centered at 735 mV was observed. This intense peak disappears during the second cycle. As the desorption potential of the SAM is at higher potentials (inset Figure S4), desorption can be excluded as origin of the peak. During the second scan, two redox peaks were observed which can be attributed to the oxidation and reduction of the TTF moiety in the SAM. But upon continuous cycling, the electrochemical signal decrease progressively. This electrochemical signal can be fully recovered if the modified electrode stands in solution without applied potential for a few minutes.

First, the intense peak observed at 930 mV during the first scan may be attributed to some considerable rearrangement in the TTFdT-SAM, due to the various options these molecules have to bind to gold. In particular the short alkyl chains and the large amount of sulfur atoms in the chain and the TTF core of 1 probably disfavor the formation of well ordered SAMs. Furthermore,

the bifunctional molecule may bind vertically with a single thiolated side chain or horizontally by binding with both terminal thiols.

Second, after important rearrangement in the SAM during the first scan, it seems that oxidation and reduction process are rather difficult to achieve. The first oxidation process appears at higher potential than for free species in solution ($E_{1/2}^1 = 0.422\text{V}$ in solution and $E_{\text{peak}}^1 = 0.685\text{V}$ in SAM). Furthermore, it appears that all oxidized species are not fully reduced during the reversible scan, as indicated by the decrease of the electrochemical signal upon cycling, and the recovery of this one after standing the modified electrode in solution without applied potential. The redox behavior of the TTFdT-SAMs is therefore rather complex. In spite of the above described current working hypothesis, the particular electrochemical behavior of the SAM functionalized electrode is not fully understood. Yet, the particular design features of the molecule were optimized for molecular place-exchange in the monolayer-protected nanoparticle arrays. In the this case, the combination of chemical and electrical characterization demonstrate a well controlled behavior.

References

- (1) X. Guo, D. Zhang, H. Zhang, Q. Fan, W. Xu, X. Ai, L. Fanc, and D. Zhu, *Tetrahedron* **59**, 4843 (2003).
- (2) J. Liao, L. Bernard, M. Langer, C. Schönenberger, and M. Calame, *Adv. Mater.* **18**, 2444 (2006).
- (3) L. Bernard, Y. Kamdzhilov, M. Calame, S. J. van der Molen, J. Liao, and C. Schönenberger, *J. Phys. Chem. C* **111**, 18445 (2007).
- (4) J. Liao, M. Mangold, S. Grunder, M. Mayor, C. Schönenberger, and M. Calame, *New J. Phys.* **10**, 065019 (2008).
- (5) V. Santhanam and R. Andres, *Nano Lett.* **4**, 41 (2004).
- (6) V. Santhanam, J. Liu, R. Agarwal, and R. Andres, *Langmuir* **19**, 7881 (2003).

(7) M. Hostetler, A. Templeton, and R. Murray, *Langmuir* **15**, 3782 (1999).

(8) R. Donkers, Y. Song, and R. Murray, *Langmuir* **20**, 4703 (2004).

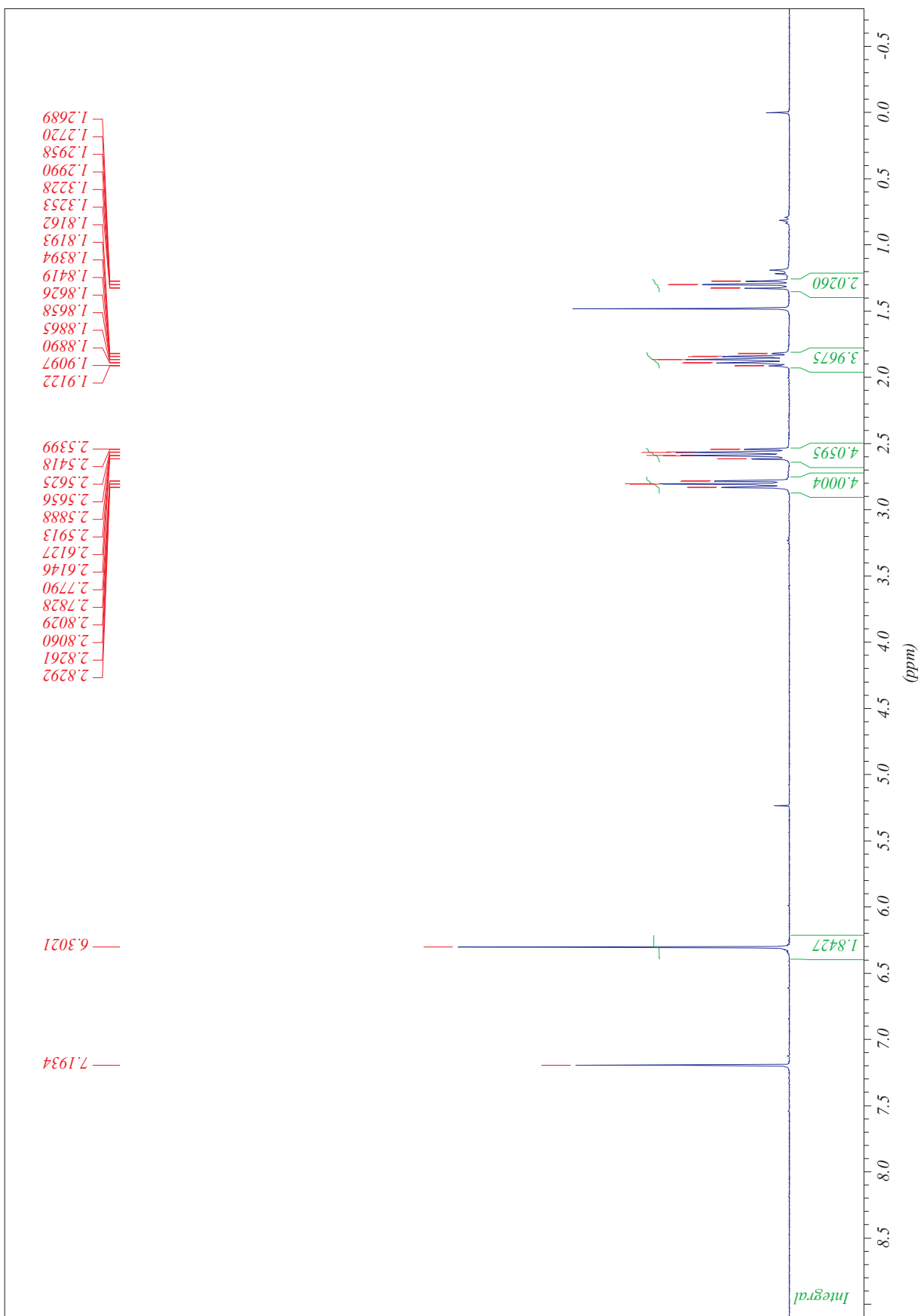


Figure S 1: ¹H NMR spectrum of compound 1

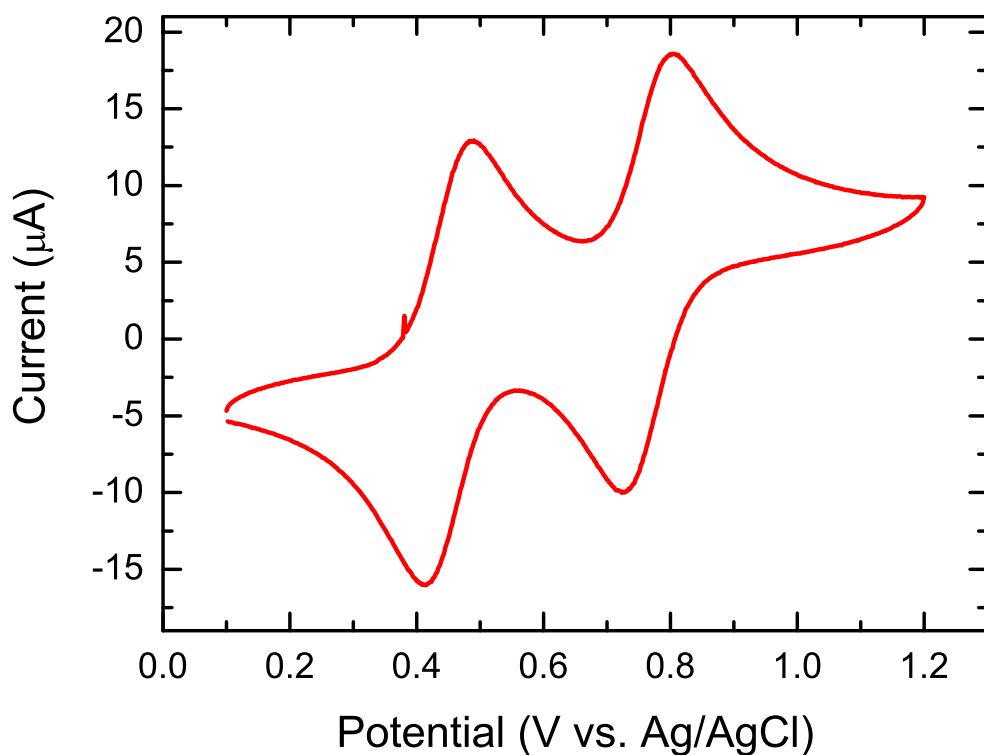


Figure S 2: **Cyclic voltammogram** of 1 mM of acetyl protected TTFdT in ACN containing 0.1M TBABF₄ as supporting electrolyte, at a scan rate of 200mVs⁻¹. The CV curve shows two clear reversible redox states for the TTFdT compound. The redox potential can be extracted from the CV curve by averaging the potential values at the reduction and oxidation peaks. We obtain a redox potential $E_{1/2}^1 = 422\text{mV vs Ag/AgCl}$ for TTF/TTF^{•+} and $E_{1/2}^2 = 747\text{mV vs Ag/AgCl}$ for TTF^{•+}/TTF²⁺.

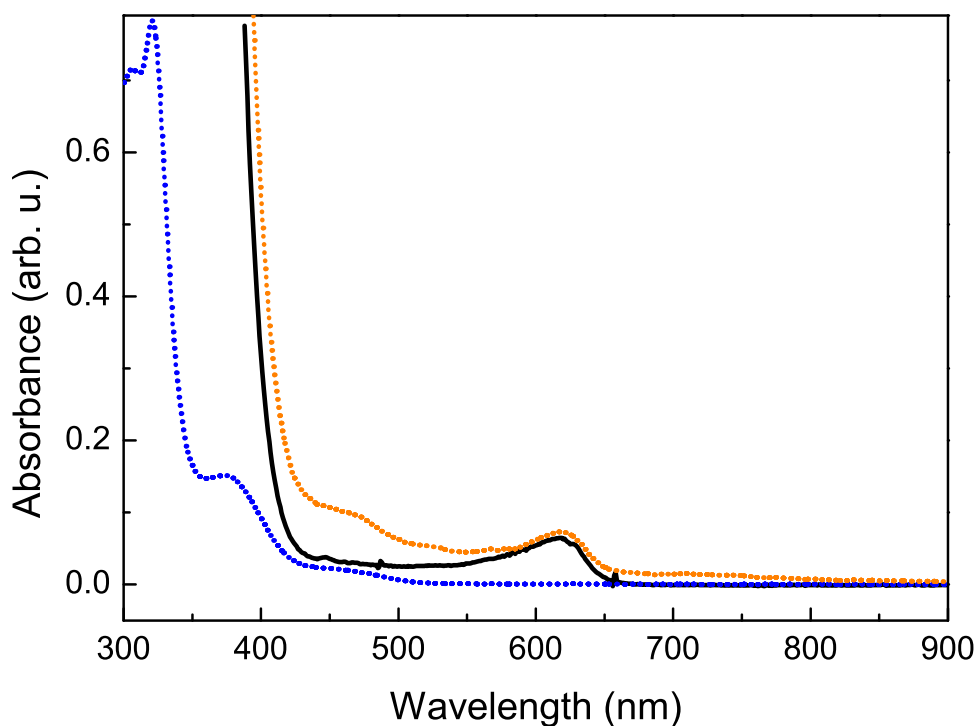


Figure S 3: **Contribution of the oxidizing and reducing agents to the UV-visible absorption spectra.** The small shoulder around 620nm visible in the spectra in Figure 2 of the manuscript is due to the presence of oxidized ferrocene. We reproduce the data from Figure 2 here. The first curve is the spectrum of a 10mM TTFdT solution in acetonitrile (dotted blue). Iron chloride was then added in excess to oxidize the TTFdT compound to the dication state, followed by the addition of ferrocene to reduce the TTFdT compound back to the neutral state (dotted orange). The third curve (black) shows the absorbance for a solution with ferrocene and iron chloride but without TTFdT molecules (same amount of iron chloride and ferrocene as for the second curve). The spectrum displays a shoulder around 620nm, similar to that in the orange curve, confirming that this feature stems from an additional absorption by oxidized ferrocene molecules.

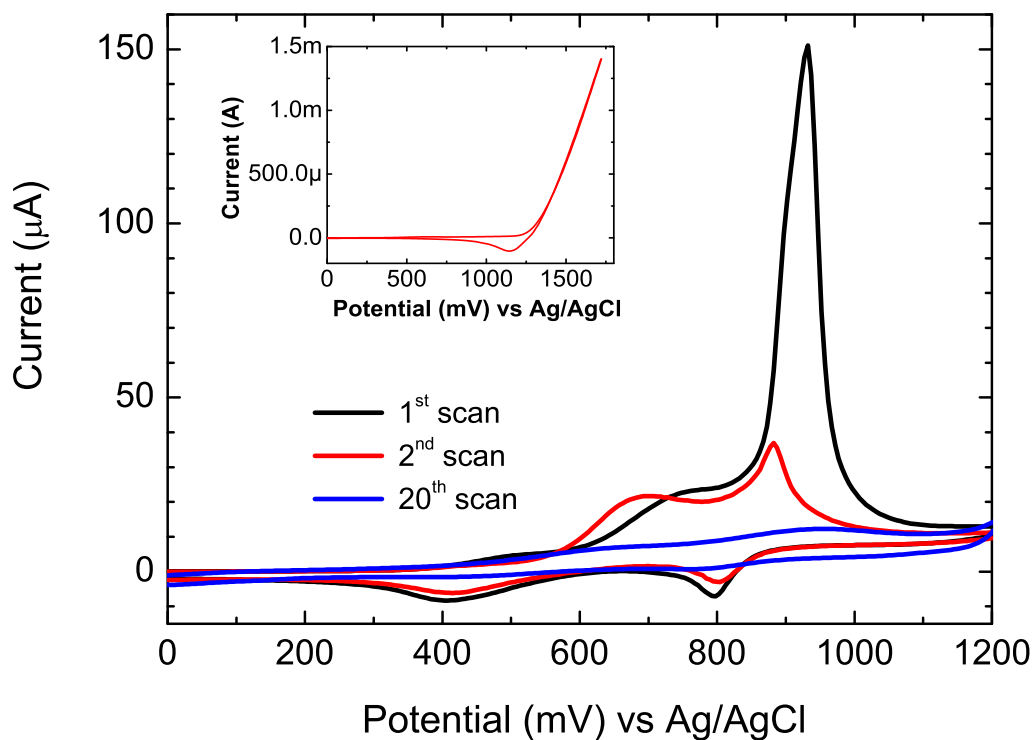


Figure S 4: **Cyclic voltammograms** of TTFdT-SAM modified gold electrodes in ACN using 0.1M TBABF₄ as supporting electrolyte. Inset: extended scan showing the desorption potential of the TTFdT-SAM.

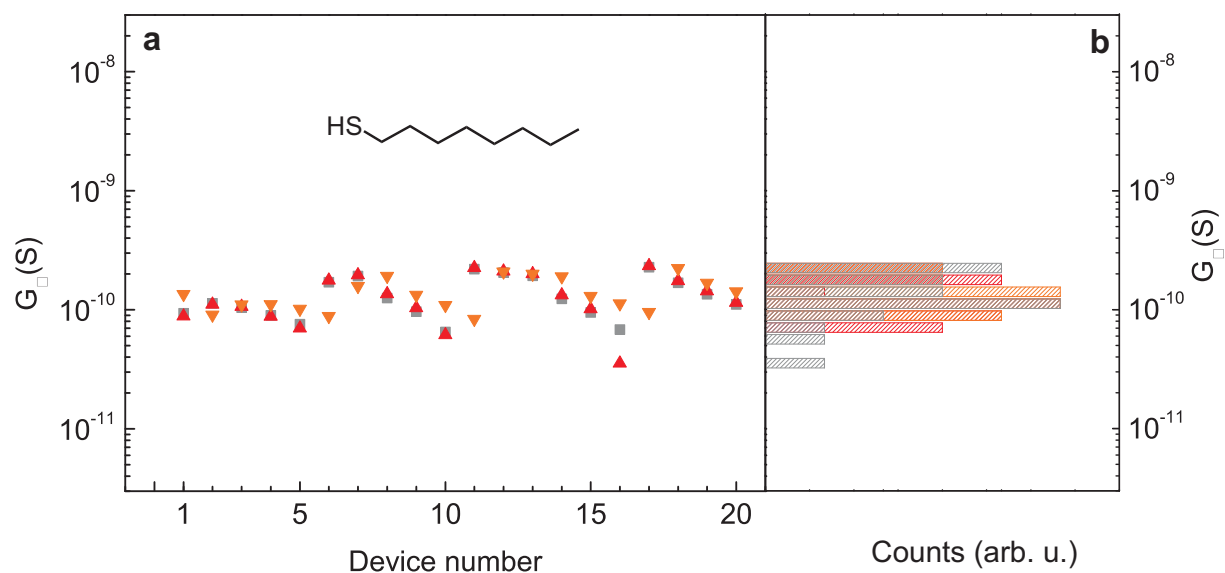


Figure S 5: **Oxidation-reduction experiment for alkane-thiol linkers C8-SH.** (a) Sheet conductance of 20 devices on one sample measured as-prepared (■), after immersion in 10ml 10mM solution of iron chloride in water for 40min (▲), and after immersion in 10ml 10mM solution of ferrocene in THF for 5 hours (▼). The conductance scale is identical to that of Figure 3a in the manuscript. (b) Histogram of the sheet conductance values shown in (a). The conductance of the devices is nearly constant upon immersion in the solution of oxidant and reductant.

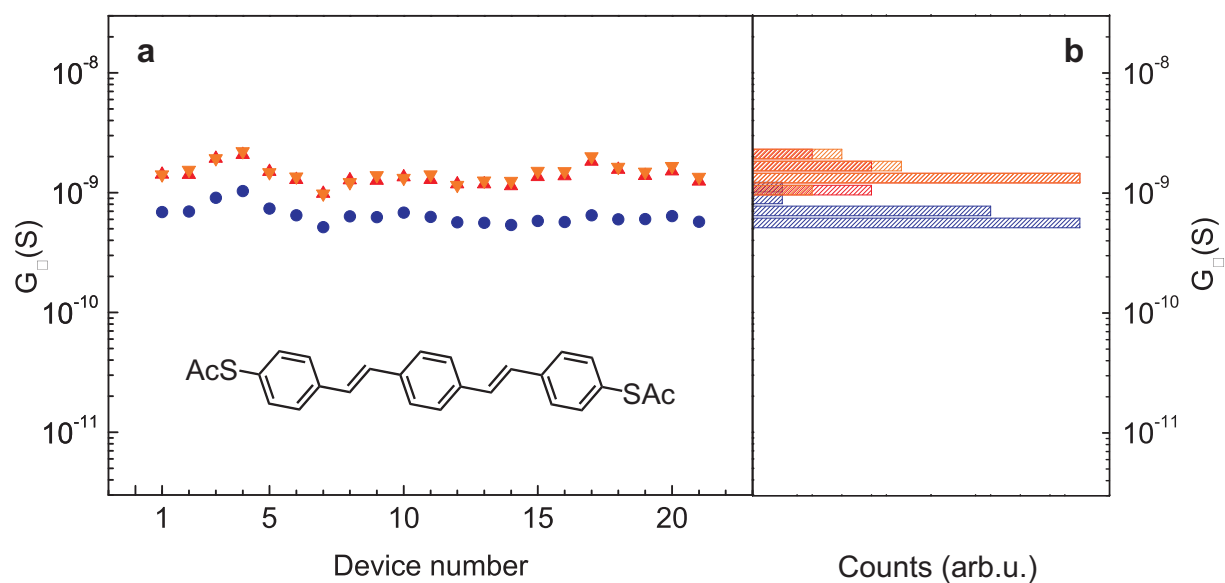


Figure S 6: **Oxidation-reduction experiment for dithiolated oligo(phenylene vinylene) compounds (OPVdT).**(a) Sheet conductance of 21 devices on one sample measured after oligo (phenylene vinylene)-dithiol exchange (●), after immersion in 10ml 10mM solution of iron chloride in water for 40min (▲), and after immersion in 10ml 10mM solution of ferrocene in THF for 16 hours (▼). The conductance scale is identical as that of Figure 3a in the manuscript. (b) Histogram of the sheet conductance values shown in (a). The conductance of the devices increases slightly upon immersion in the oxidant. This is attributed to a coordination of the unbound thiol end-groups of the OPVdT with the iron species present in the oxidant. No change is observed in the reducing solution.